JOURNAL OF AQUATIC FOOD PRODUCT TECHNOLOGY
https://doi.org/10.1080/10498850.2021.1961962

Experimental and Simulation Study of Drying Skipjack Tuna with a Modified Microwave Drying System

Saysunee Jumrat[a,b], Teerasak Punvichai[a,c], Seppo Karrila[b], Mudtorlep Nisoa[d], and Yutthapong Pianroj[a,b]

[a]Integrated High-Value Oleochemical Research Center, Prince of Songkla University Suratthani Campus, Surat Thani, Thailand; [b]Faculty of Science and Industrial Technology, Prince of Songkla University Suratthani Campus, Surat Thani, Thailand; [c]Faculty of Innovation Agriculture and Fisheries Establishment Project, Prince of Songkla University, Suratthani Campus, Surat Thani, Thailand; [d]Molecular Technology Research Unit, School of Science, Walailak University, Nakhon Si Thammarat, Thailand

ABSTRACT

A microwave (MW) drying system was built for drying skipjack tuna. It was composed of waveguide and cavity, and a modification to the high-voltage power supply using a power electronic device to control the phase of AC input voltage to a high-voltage transformer. The calibration of the MW power enables tuning the power to be used for drying skipjack tuna. The experimental set-up was studied drying kinetics: time profiles of temperature and moisture content (%MC). The temperature was measured using a thermopile thermometer, which was connected to the microcontroller and the PC via an RS232 port. The %MC was monitored gravimetrically. The experimental results and the simulation results from finite element method computations were compared by assessing the coefficient of determination (R^2) and the root-mean-square-error (RMSE). Finally, empirical and semi-theoretical models were fit to the experimental results of moisture ratio and evaluated for best fit using R^2 and *RMSE*.

KEYWORDS

Microwave drying; dried fish; skipjack tuna; microwave power supply

Introduction

Thailand produces many fishery products, especially in the provinces by the Gulf of Thailand. The commercially important skipjack tuna (*Katsuwonus pelamis*) fish is distributed both in the off-shore waters and in the open seas of tropical and temperate regions around the world (Pornchaloempong et al. 2012). It is one of the most important fish species among those cooked and canned in Thailand (Klomklao et al. 2004). The preservation of a catch to maintain quality and prevent spoilage uses cooling and drying techniques. Drying can preserve the fish because removing the moisture inactivates enzymes that are essential for bacterial growth (Bala and Mondol 2001; Bellagha et al. 2002; Duan et al. 2011). Traditional drying utilizes heat from the sunshine in the dry season or heat from burning wood during the rainy season. While this has been done since time immemorial for agricultural products, unfortunately such natural drying is very slow and exposes the fish to uncontrolled environmental effects such as weather uncertainties, requires a large drying area, and may lead to contamination by dust and pathogens.

During the past decade, there have been many successful studies on microwave (MW) utilization for drying or heating food and other dielectric materials. Its advantages include reduced shrinkage, lower bulk density, higher rehydration ratio, fast dehydration rate, and overall fast processing due to the volumetric heating, as well as convenience and energy savings over traditional drying (Aydogdu

CONTACT Yutthapong Pianroj yutthapong.p@psu.ac.th Integrated High-Value Oleochemical Research Center, Prince of Songkla University Suratthani Campus, 31 Moo 6, Makham-Thea, Muang, Surat Thani 84000, Thailand.

et al. 2015; Duan et al. 2010; Horuz and Maskan 2015; Pu and Sun 2015, 2016, 2017). Therefore, interest in this type of study has increased rapidly, as evidenced by many publications, including excellent review papers (Guo et al. 2017; Marra et al. 2009; Sosa-Morales et al. 2010) and books (Datta and Anantheswaran 2001; Meredith 1998; Metaxas and Meredith 1983; Schubert and Regier 2005). MW drying of fish has also been studied. Duan et al. (2011), (2005)) and Darvishi et al. (2013) used MW at 200–800 W power combined with hot air to study the drying characteristics of fresh tilapia fillet, bighead carp, and sardine. They found that hot air-MW drying technology can decrease the drying time and improve the product quality. Kipcak (2017) and Kipcak and İsmail (2021) studied the MW drying kinetics of mussels (*Mytilus edulis*) and samples of fish, chicken, and beef. A suitable MW power was 360 W, and the effective moisture diffusivity was of the order 10^{-8}–10^{-7} m^2/s; moreover, Kipcak et al. (2019) and Sevim et al. (2019) used infrared as a heat source for studying the drying kinetics of mussels.

Extensive studies have been done using conventional household MW ovens to dry fish. A disadvantage of this technology is the single power level, so that heating is regulated by an ON/OFF type control. Cheng et al. (2006a, 2006b) controlled the MW power supply by using a phase-control of the input voltage and evaluated the effects of two alternative power control methods, namely phase control and cycle control. They found that phase-controlled power could be used for quasi-continuous power regulation, maximizing the power efficiency and allowing decrease of MW output power.

The novel methods and objectives of this study are summarized as follows. The drying set-up had a continuous MW power control and air exchange for drying. The study modified a MW drying system so that it was appropriate for drying fish (not for cooking the fish) at a low 60 W power (maintaining temperatures below 40°C) for 160 min. Moreover, simulations were used to evaluate the relation between MW output power and drying characteristics. Thus, this paper is organized as follows: fundamental theories of MW drying for food materials are briefly described in the next section. The experiments and simulations of MW drying skipjack tuna are described in Section 3. The experimental and simulation results are presented in Section 4, and a summary is given in the last section.

Materials and methods

Experimental setup

Commonly, a MW drying or heating system is composed of the MW source (magnetron), a high-voltage power supply, a waveguide, and the MW cavity. The magnetron is of commercial type, producing the MW frequency 2.45 GHz. On supplying 3 V and 11A to the filament cathode of the magnetron, electrons are emitted from the hot cathode. These electrons are influenced by the magnetic field of a permanent magnet and by the electric field between the cathode and the anode, induced by an external high-voltage power supply. The threshold output voltage for emitting MWs is about 4,000 V. As the output voltage is increased from 4,000 to 6,000 V, the MW power is altered. The modified high-voltage power supply (Pianroj et al. 2006) was developed based on these facts, by connecting two high-voltage transformers in series, while the control unit for phase control of the input AC voltage was installed into the controller circuit. The main device is a high-power TRIAC, utilized to adjust the input voltage properly for the two transformers.

The output of the lower transformer is fixed at 3,000 V, whereas the upper transformer in this system produces an output voltage between 1,000 and 3,000 V. After that, the MW power calibration was performed in the test set-up shown in Figure 1.

We assume no energy loss on conversion of MW power (P_{MW}) to heat in the water. The MW power is therefore calculated as follows (Cao et al. 2018).

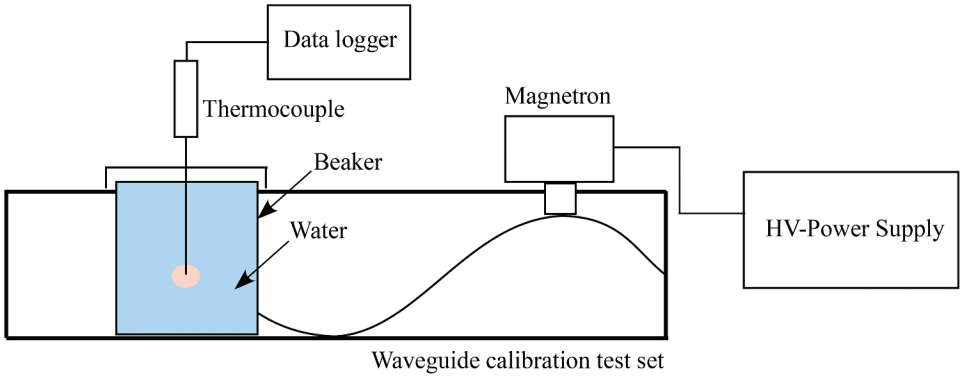

Figure 1. Schematic of the experimental setup for microwave power calibration.

$$P_{\mathrm{MW}} = \frac{\rho V c_p \Delta T}{t} = \frac{4,178 V \Delta T}{t} \tag{1}$$

where ρ is the density of water, c_p (4,178J/(Kg℃) is specific heat capacity of water, t is time (s), V is the water volume (m^3), and ΔT is the temperature difference of the water after absorbing MW power for t seconds. Figure 2 shows that P_{MW} increases exponentially with the input voltage (V_{in}). The fit by exponential relationship, $P_{\mathrm{MW}} = 0.252e^{0.031V_{in}}$ gave a coefficient of determination of $R^2 = 0.995$, and the threshold input voltage for emitting MW power is about 100 V.

For effective transmission of MW power to the fish, the waveguide and cavity were designed carefully and are shown in Figure 3. The rectangular waveguide, made of stainless steel, was designed for TE_{01} mode. It had a width of 8 cm and a height of 4 cm. The cavity was designed for multimode operation. The size was 32 × 40 × 30 cm (height × width × length). The walls of the cavity were

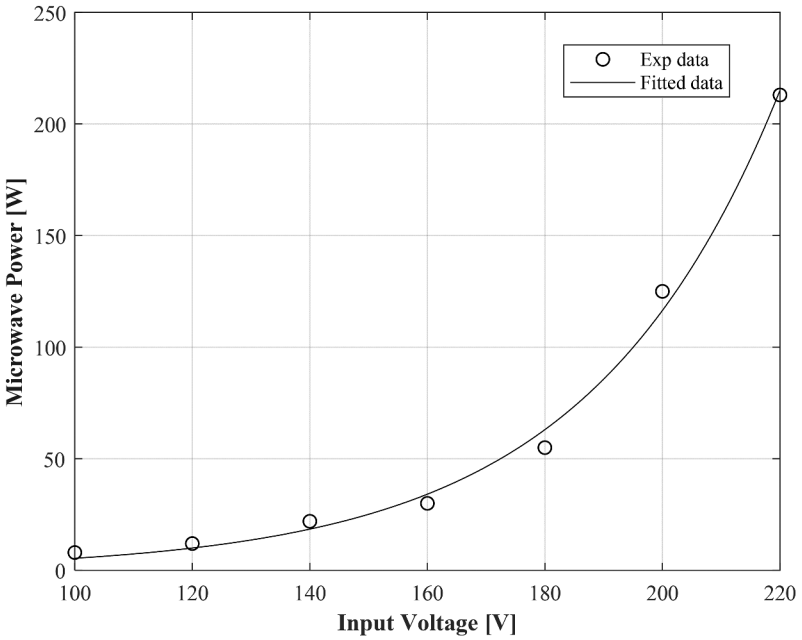

Figure 2. Calibration curve between the input voltage (V_{in}; V) versus the microwave power (P_{MW}; W).

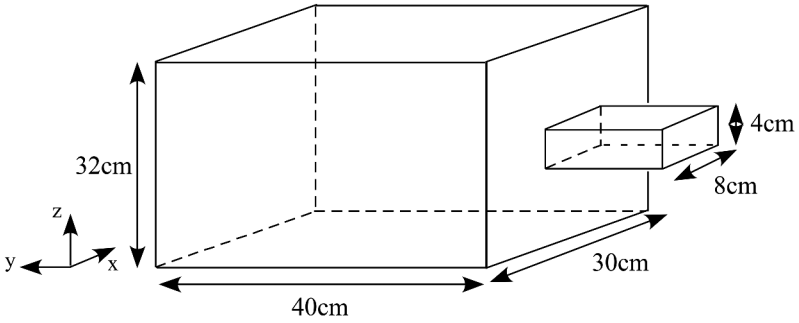

Figure 3. Schemetic diagram of the multimode cavity and waveguide.

perforated stainless steel, with an array of small circular apertures of 3 mm diameter. This enables the in-out circulation of air to and from the cavity.

Raw skipjack tuna (0.8 kg) was obtained from the local seafood market. It was cut along the back, spread out, and the viscera were removed. The thickness of the fish was on average 1.8 cm, width 6.0 cm, and length 12.0 cm. This process was called pre-drying, and is shown in Figure 4. The initial moisture content (MC) of skipjack tuna was 71.4% (wet basis) at room temperature 26.5℃, as determined by the thermogravimetric method with infrared moisture analyzer SARTORIUS MA35. The MC during drying skipjack tuna (at a given time t) can be transformed to be the dimensionless moisture ratio (MR) as follows:

$$\mathrm{MR} = \frac{M_t - M_{eq}}{M_i - M_{eq}} \tag{2}$$

where M_t is the total moisture content at drying time t, M_i is the initial moisture content, and M_{eq} is the equilibrium moisture content (46.5%, estimated at the end of a drying run).

In this study, the drying kinetics were evaluated based on measured surface temperature and the percentage moisture content. The surface temperature measurement could be determined by inserting the infrared sensor inside a waveguide calculated to avoid the waves reaching the sensor. This technique was used in the prior works by Monteiro et al. (2015), (2020). The experimental set-up used for these observations is shown in Figure 5. The infrared (IR) thermometer was a smart thermopile sensor with an integrated signal processing circuit, model A2TPMI 334-L5.5 OAA 120 from PerkinElmer (Waltham, MA, USA), and the digital balance was model PG2002-S from Mettler-Toledo (Toledo, OH, USA), with the skipjack tuna hung from it by a nylon string. The IR thermometer had temperature range from −20 to 120℃, and an integrated, calibrated ambient temperature sensor, so the single output was ambient temperature compensated and with rapid reaction time. It was connected to the 10-bit Analog to Digital (A/D) module of Micro-Controller Unit (MCU; PIC-16F877 from Microchip), and then the surface temperature signal was logged by a personal computer (PC) via

Figure 4. Pre-drying treatment of skipjack tuna.

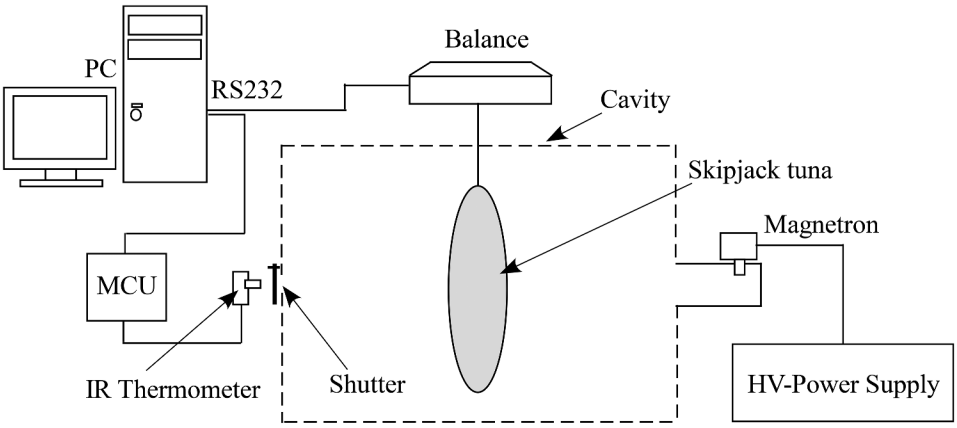

Figure 5. Schematic of the experimental setup for microwave drying of skipjack tuna.

the serial port (RS232). The balance was connected to an RS232 port like the IR thermometer to collect in real-time the sample weight during a drying run.

The MW power 60 W was used to dry the fish and to study the drying kinetics. The experiment began by hanging the pre-treated fish inside the cavity with the nylon string. The outside end of the nylon string was connected to the balance for measuring the weight. The frequency of logging the weight was 1 per second, and the drying time was 160 min. The surface temperature was measured every 15 min: the MW power was switched OFF, the shutter was opened, and the IR thermometer performed the measurement. This took about 10 seconds per measurement, and it was assumed that the surface temperature did not change during the measurement. The MW power had to be switched OFF to avoid MW interference with the IR signal.

Simulation setup

In this section, the simulation, which was based on a mathematical model, was formulated to predict the drying related parameters, such as the surface temperature and the percentage of moisture as functions of the drying time, for comparison with the experimental data. The simulation was coupled with an analysis of the electro–thermal interactions and the diffusion mass transport. The system of governing equations with initial and boundary conditions was solved numerically in a three-dimensional (3D) model with the finite element method (FEM) in COMSOL^{TM} Multiphysics software.

Governing equations

MW heating or drying is based on interactions between the electromagnetic waves in frequency range from 300 MHz to 300 GHz and a dielectric material, such as food or a biological product. The MW propagation is described by Maxwell's equations. For the frequency-domain electromagnetic field in the rectangular MW oven (waveguide and cavity), the following equation was solved for the electric field ($\vec{E}$).

$$\times \left(\mu_r^{-1} \quad \times \vec{E}\right) - k_0^2\left(\varepsilon_r - \frac{j\sigma}{\omega\varepsilon_0}\right)\vec{E} = 0 \tag{3}$$

where μ_r is the relative permeability, $j = \sqrt{-1}$, σ is the conductivity, ω is the angular frequency, ε_r is the relative permittivity, and ε_0 is the permittivity of free space. In this equation, the relative permittivity is a complex quantity, generally used to describe the dielectric properties that influence reflection of electromagnetic waves at interfaces and the attenuation of wave energy within materials. The relative

complex permittivity relates to the free space permittivity and is given by the following equation (Sosa-Morales et al. 2010).

$$\varepsilon_r = \varepsilon_r' - j\varepsilon_r'' \tag{4}$$

where ε_r' and ε_r'' are the dielectric constant and the dielectric loss factor, respectively. Food materials convert electric field energy at MW frequency into heat. The temperature of food due to MW heating can be calculated from

$$\rho C_p \frac{dT}{dt} = \quad \cdot (k \quad T) + Q_{\mu w} \tag{5}$$

where ρ is the density of the food material [kg/m^3], C_p is the specific heat of food material [J/kg · K], k is the thermal conductivity of food material [W/m · K], dT/dt is the time rate of temperature increase [℃/s], and $Q_{\mu w}$ is the heat source from MWs. $Q_{\mu w}$is proportional to the relative dielectric loss factor and square of electric field strength, so it can be calculated from (Metaxas 1996)

$$Q_{\mu w} = 0.5\omega\varepsilon_0\varepsilon_r'' E^2 \tag{6}$$

where E is the root mean square (RMS) of electric field [V/m]. When the temperature of food material increases, the moisture inside gets more molecular kinetic energy, moving the moisture from inside to outside the food material. This moisture transfer dries the sample, and the diffusion is described by Fick's law as shown here

$$\frac{\partial c}{\partial t} + \quad \cdot (-D \quad c) = 0 \tag{7}$$

where c is the moisture concentration, and D is the diffusion coefficient [m^2/s].

Initial and boundary conditions

For electromagnetic heating, the waveguide and cavity of MW oven are metallic, with the dimensions shown in Figure 3. Therefore, the boundary conditions in the simulation model were set for perfect electric conductors, as

$$\vec{n} \times \vec{E} = 0 \tag{8}$$

The MW power at 60 W and frequency 2.45 GHz exited from the rectangular waveguide opening in TE_{01} mode.

Regarding the heat transfer, the latent heat taken by evaporation of water during drying skipjack tuna generates a heat flux out of the sample; thus, the boundary conditions of the drying skipjack tuna were set as

$$\vec{n} \cdot (k \quad T) = h_T(T_{air} - T) + \lambda\vec{n} \cdot (D \quad c) \tag{9}$$

where h_T is the heat transfer coefficient [W/(m^2 · K)], T_{air} is the surrounding air temperature (30℃), λ is the molar latent heat of vaporization [J/mol], D is the moisture diffusion coefficient in the drying skipjack tuna [m^2/s], and c is moisture concentration [mol/m^3].

The boundary conditions for diffusion were

$$\vec{n} \cdot (D \quad c) = k_c(c_b - c) \tag{10}$$

where k_c refers to the mass transfer coefficient [m/s], and c_b denotes the outside air moisture concentration [mol/m^3]. The diffusion coefficient and the mass transfer coefficient are

$$D = \frac{k_m}{\rho C_m}, k_c = \frac{h_m}{\rho C_m} \tag{11}$$

where C_m equals the specific moisture capacity, k_m refers to the moisture conductivity [kg/(m · s)], and h_m denotes the mass transfer coefficient in the mass unit [kg/(m^2 · s)].

In order to simulate this system, the following assumptions were adopted.

(1) The skipjack tuna model was created based on ellipsoid geometry, with semiaxes (a, b, and c; in the Cartesian x–y–z coordinate system) 6.0, 1.8, and 12.0 cm, respectively (a symmetric ellipsoid).
(2) The material had homogenous properties, without differences between backbone, loin, and skin.
(3) The density of skipjack tuna fish was only an apparent density, because the volume of the fish was for head, bone, flesh, intestine, etc. and cavity volume, which are reported by Pornchaloempong et al. (2012).

A summary of the parameters in initial conditions and material properties is given in Table 1.

A simulation with the three-dimensional model for this study is shown in Figure 6a and free tetrahedral meshing had 101,475 domain elements, 6,464 boundary elements, and 547 edge elements, as depicted in Figure 6b.

Empirical modeling of drying process

Three commonly used mathematical models for the moisture ratio during thin layer drying are given in Table 2, and these were assessed for describing the drying kinetics of skipjack tuna. These empirical and semi-theoretical models were fit to the experimental results using nonlinear regression. The goodness of the model fit to the experimental results was evaluated by using the coefficient of determination (R^2) and the root-mean-square-error ($RMSE$). The goodness of fit improves as R^2 increases up to one and as $RMSE$ approaches zero. The nonlinear regression fits with the three tested models are shown in Table 2.

Table 1. Summary of initial conditions and properties applied in the model.

Parameter	Notation [Unit]	Value
Dielectric constant (Liu et al. 2012)	ε'	$-2.59e^{-3} \times T^2 + 1.07e^{-1} \times T + 42.9$; [℃]
Dielectric loss factor (Liu et al. 2012)	ε''	$-1.08e^{-4} \times T^2 + 2.90e^{-1} \times T + 14.1$; [℃]
Density of fish (Pornchaloempong et al. 2012)	ρ [kg/m^3]	1,072.86
Specific heat (Zhang et al. 2002)	C_p [J/kg · K]	3,505
Thermal conductivity (Zhang et al. 2002)	k [W/m · K]	$0.09+(5.01 \times x_w)+(5.05e^{-4} \times x_w \times T)$
Heat transfer coefficient	h_T [W/m^2 · K]	7.18
Mass fraction of water/MC	x_w	0.71
Mass transfer coefficient in mass unit	h_m [kg/m^2 · s]	$4.72e^{-7}$
Diffusion (Zhang et al. 2001)	D [m^2/s]	$1.49e^{-7}$
aInitial moisture concentration	c_0 [mol/m^3]	42,443
aAir moisture concentration	c_b [mol/m^3]	1,188.90
specific moisture capacity (Chen et al. 1999)	C_m	0.003
Mass transfer coefficient	k_c [m/s]	$1.47e^{-7}$
Molar latent heat of vaporization (Chen et al. 1999)	λ [J/mol]	41,400
Surrounding air temperature	T_{air} [℃]	30
Initial temperature of fish	T_0 [℃]	26.2

[a]Remark $c_0 = (MC \times \rho)/M\_H_2O$; $c_b = (0.02 \times \rho)/M\_H_2O$, where M_H_2O is the molecular weight 0.018 kg/mol of water, and $k_m = D \times \rho \times C_m$

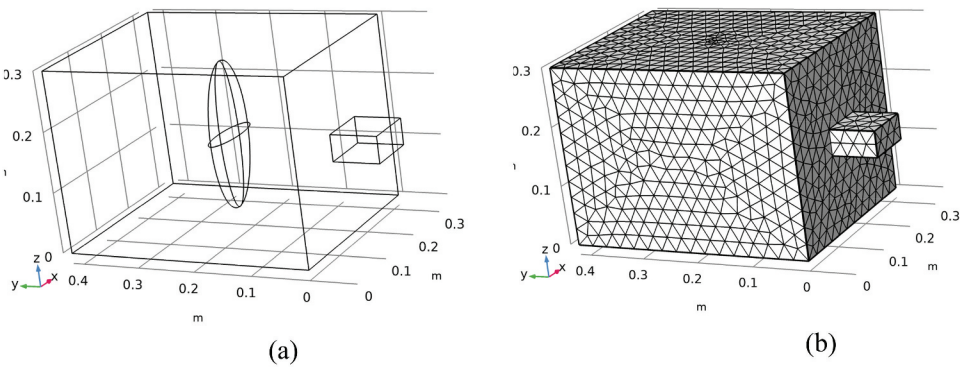

Figure 6. The 3D model of drying skipjack tuna with a modified MW drying system: (a) the wireframe rendering, (b) 3D domain with free tetrahedral meshing.

Table 2. Goodness of fit statistics for models fit to microwave dry skipjack tuna fish.

Model Name	Model	Model constants	R^2	*RMSE*
Page (Pianroj et al. 2018)	$MR = \exp(-kt^n)$	k = 0.024, n = 0.693	0.969	0.028
Wang and Singh (Arslan and Musa Özcan 2010)	$MR = 1 + bt + at^2$	a = 1.745e-5, b = −0.006	0.917	0.047
Parabolic (Sharma and Prasad 2001)	$MR = c + bt + at^2$	a = 1.750e-5, b = −0.006 c = 0.911	0.964	0.032

Results and discussion

As a result of the high-voltage power supply modification, which was described in Section 2.1, an input voltage around 180 V was supplied to generate the MW power 60 W for making dried skipjack tuna with a drying time of 160 min. The experiments (triangles) and simulation (solid line) are shown in Figure 7. In the first period of drying for around 40 min, the temperature in experimental results of the top panel in Figure 8 steeply increased, which relates to the rapid decrease of moisture in skipjack tuna seen in the bottom panel of Figure 8. This phenomenon comes from the free water in skipjack tuna, which absorbs the MW energy and converts it to heat, so there is rapid volumetric heating. Thus, moisture in the form of free water strongly increased kinetic molecular energy, causing evaporation and transport to the skipjack tuna surface, as was found in Arballo et al. (2010) and Li et al. (2011), and the moisture ratio rapidly decreased. After the first 40 min, the temperature slowly increased due to the bound water in the skipjack tuna, which had more structural bonding than the free water, and the molecules could not escape as vapor. This continued until the end of drying at 160 min. The same behavior has been found in prior studies that have divided the drying into three stages, namely heating up, constant rate drying, and falling rate drying (Bal et al. 2010). Moreover, simulations were carried out for the same location on sample as the surface temperature measurement. To quantify the comparison between simulations and experimental results, the coefficient of determination and RMSE were calculated to assess the differences between simulated and experimental results. In this work, the R^2 and *RMSE* are defined, respectively, by Equations (12) and (13).

$$R^2 = 1 - \frac{\sum_i^N \left(y_{\exp_i} - y_{\mathrm{sim}_i}\right)^2}{\sum_i^N \left(y_{\mathrm{sim}_i} - \bar{y}_{\mathrm{sim}}\right)^2} \tag{12}$$

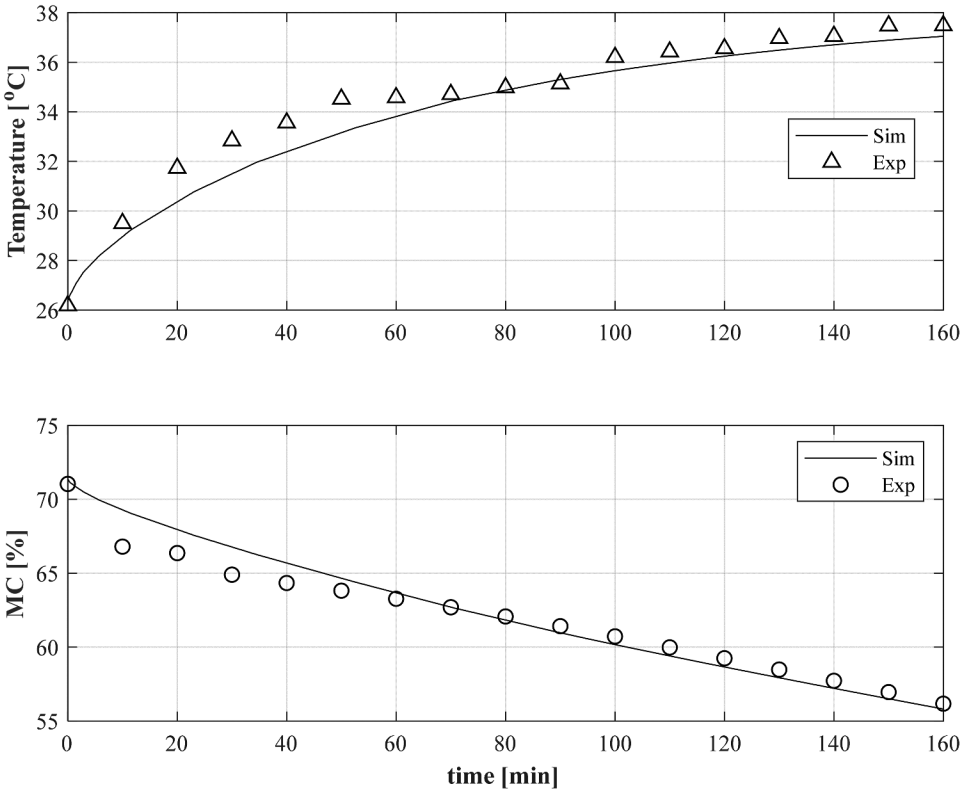

Figure 7. Drying kinetics of microwave drying skipjack tuna. The top panel shows the surface temperature as a function of drying time, and the bottom panel is the % moisture content (%MC) as a function of drying time.

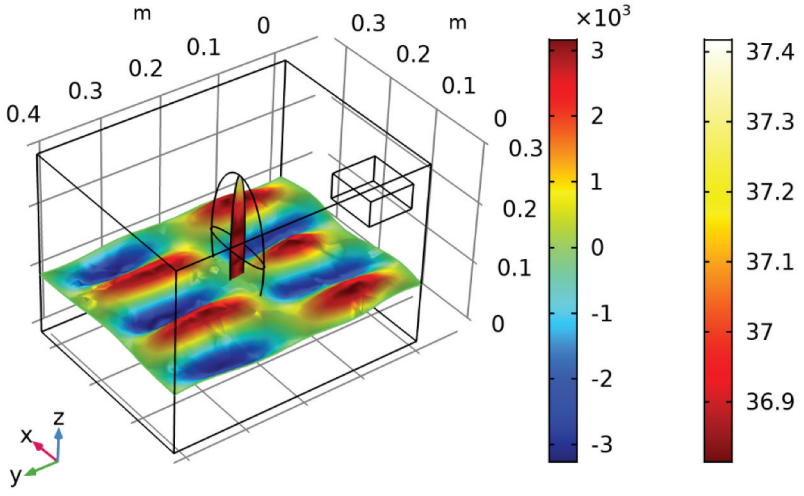

Figure 8. Plot of electric field (V/m) pattern in *x*–*y* plane and temperature plot in the skipjack tuna model along the *y*–*z* plane.

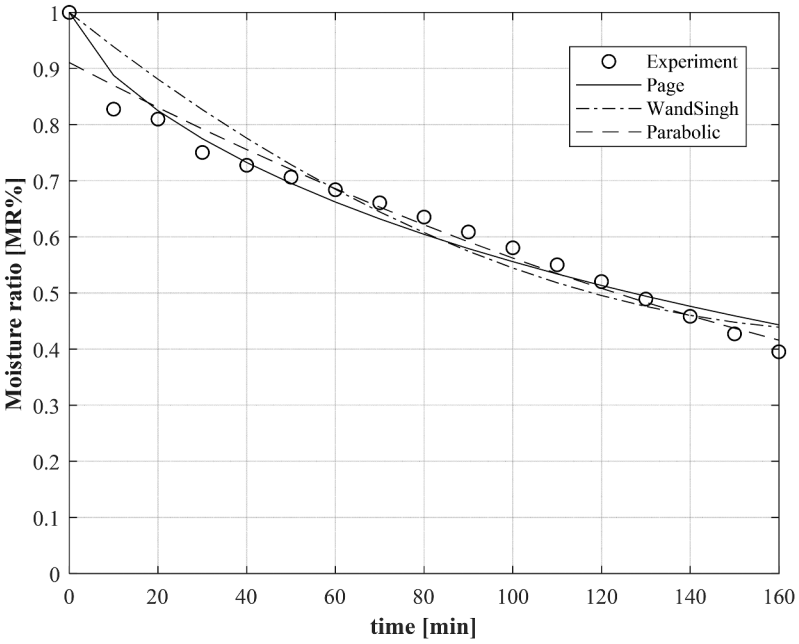

Figure 9. Plot of the experimentally observed moisture ratio (MR%) as a function of drying time and the fitted models from Table 2.

$$RMSE = \sqrt{\frac{1}{N}\sum_{i}^{N}\left(y_{\exp_i} - y_{\mathrm{sim}_i}\right)^2} \tag{13}$$

where $y_{\exp_i}$ is the i^{th} data point of the experimental results, y_{sim_i} is the corresponding data point of the simulation results, and $\bar{y}_{\mathrm{sim}}$ is the average of all N simulated data points. The R^2 and $RMSE$ for temperature were 0.942 and 0.745, respectively; and for %MC, they were 0.933 and 1.012, respectively. This indicates that the simulations matched the experimental results well. However, the simulations had comparatively large differences from the experimental results for the first drying period, due to quick removal of the free water from skipjack tuna.

Figure 8 shows the electric field distribution in the x–y plane and the temperature over a slice of skipjack tuna in the y–z plane at the end of drying (160 min) from the simulation. The electric field inside the MW cavity had a standing-wave pattern, which is from interference effects with an amplitude $\pm$ 3,000 V/m; moreover, the temperature had nonuniform distribution due to the thickness of the skipjack tuna along the y–z plane.

To fit the moisture ratio data from skipjack tuna drying using MWs, three models were tested, as shown in Table 2. The quality of fit for each model was assessed from the coefficient of determination and from RMSE. The best model describing the thin-layer drying characteristics of skipjack tuna was chosen based on the highest R^2 and the least $RMSE$. Table 2 shows that the best fit model is Page, followed by Parabolic, and Wang and Singh models in this rank order, and the fits by each model are shown in Figure 9.

Conclusion

A modification of the high-voltage power supply for MW drying was successfully developed to make dried skipjack tuna. The calibration results show the MW power range 5.4–216.3 W for manipulated input voltages of 100–220 V. The MW drying system consists of waveguide and cavity, made of solid and mesh stainless steel, respectively. The experimental results showed rapidly increasing temperature

and steeply decreasing moisture content in the first 40 min of drying, due to free water in the fish. During the remaining drying until the end of a drying run, both temperature and %MC slowly approached steady states as the bound water in skipjack tuna was removed. Simulations were carried out and verified using the coefficient of determination and the root-mean-square-error to quantify fit with experimental results. The R^2 and *RMSE* were 0.942 and 0.745 for temperature and 0.933 and 1.012 for %MC, respectively. The best fit empirical mathematical model for the moisture ratio was the Page model (R^2 = 0.969; *RMSE* = 0.028), followed by Parabolic model (R^2 = 0.964; *RMSE* = 0.032), and Wang and Singh model (R^2 = 0.917; *RMSE* = 0.047).

Acknowledgments

Authors gratefully thank the financial support from Research Development Office (RDO), Prince of Songkla University, Hat-Yai campus, and from Prince of Songkla University, Surat-Thani campus under Integrated High-Value Oleochemical Research Center.

Disclosure statement

No potential conflict of interest was reported by the author(s).

ORCID

Saysunee Jumrat http://orcid.org/0000-0003-2048-2003
Teerasak Punvichai http://orcid.org/0000-0001-6159-3848
Seppo Karrila http://orcid.org/0000-0002-2818-6746
Yutthapong Pianroj http://orcid.org/0000-0002-4500-1045

References

Arballo J.R., Campañone L.A., Mascheroni R.H. 2010. Modeling of Microwave Drying of Fruits. Drying Technol. 28 (10):1178–84.
Arslan D., Musa Özcan M. 2010. Study the Effect of Sun, Oven and Microwave Drying on Quality of Onion Slices. LWT - Food Sci Technol. 43(7):1121–27.
Aydogdu A., Sumnu G., Sahin S. 2015. Effects of Microwave-Infrared Combination Drying on Quality of Eggplants. Food Bioprocess Tech. 8(6):1198–210.
Bal L.M., Kar A., Satya S., Naik S.N. 2010. Drying Kinetics and Effective Moisture Diffusivity of Bamboo Shoot Slices Undergoing Microwave Drying. Int J Food Sci Technol. 45(11):2321–28.
Bala B.K., Mondol M.R.A. 2001. Experimental Investigation on Solar Drying of Fish Using Solar Tunnel Dryer. Drying Technol. 19(2):427–36.
Bellagha S., Amami E., Farhat A., Kechaou N. 2002. Drying Kinetics and Charecteristic Drying Curve of Lightly Salted Sardine (Sardinella Aurita). Drying Technol. 20(7):1527–38.
Cao H., Fan D., Jiao X., Huang J., Zhao J., Yan B., Zhou W., Zhang W., Zhang H. 2018. Effects of Microwave Combined with Conduction Heating on Surimi Quality and Morphology. J Food Eng. 228:1–11.
Chen H., Marks B.P., Murphy R.Y. 1999. Modeling Coupled Heat and Mass Transfer for Convection Cooking of Chicken Patties. J Food Eng. 42(3):139–46.
Cheng W.M., Raghavan G.S.V., Ngadi M., Wang N. 2006a. Microwave Power Control Strategies on the Drying Process I. Development and Evaluation of New Microwave Drying System. J Food Eng. 76(2):188–94.
Cheng W.M., Raghavan G.S.V., Ngadi M., Wang N. 2006b. Microwave Power Control Strategies on the Drying Process II. Phase-controlled and Cycle-controlled Microwave/air Drying. J Food Eng. 76(2):195–201.
Darvishi H., Azadbakht M., Rezaeiasl A., Farhang A. 2013. Drying Characteristics of Sardine Fish Dried with Microwave Heating. J Saudi Soc Agr Sci. 12(2):121–27.
Datta A.K., Anantheswaran R.C. 2001. Handbook of Microwave Technology for Food Applications. New York (NY): M. Dekker.
Duan X., Zhang M., Mujumdar A.S., Wang S. 2010. Microwave Freeze Drying of Sea Cucumber (Stichopus Japonicus). J Food Eng. 96(4):491–97.
Duan Z., Zhang M., Hu Q., Sun J. 2005. Characteristics of Microwave Drying of Bighead Carp. Drying Technol. 23 (3):637–43.

Duan Z.-H., Jiang L.-N., Wang J.-l., Yu X.-Y., Wang T. 2011. Drying and Quality Characteristics of Tilapia Fish Fillets Dried with Hot Air-microwave Heating. Food Bioprod Process. 89(4):472–76.
Guo Q., Sun D.-W., Cheng J.-H., Han Z. 2017. Microwave Processing Techniques and Their Recent Applications in the Food Industry. Trends Food Sci Technol. 67:236–47.
Horuz E., Maskan M. 2015. Hot Air and Microwave Drying of Pomegranate (Punica Granatum L.) Arils. J Food Sci Technol. 52(1):285–93.
Kipcak A.S. 2017. Microwave Drying Kinetics of Mussels (Mytilus Edulis). Res Chem Intermed. 43(3):1429–45.
Kipcak A.S., Doymaz I., Derun E.M. 2019. Infrared Drying Kinetics of Blue Mussels and Physical Properties. Chem Ind Chem Eng Q. 25(1):1–10.
Kipcak A.S., İsmail O. 2021. Microwave Drying of Fish, Chicken and Beef Samples. J Food Sci Technol. 58(1):281–91.
Klomklao S., Benjakul S., Visessanguan W. 2004. Comparative Studies on Proteolytic Activity of Splenic Extract from Three Tuna Species Commonly Used in Thailand. J Food Biochem. 28(5):355–72.
Li Z.Y., Wang R.F., Kudra T. 2011. Uniformity Issue in Microwave Drying. Drying Technol. 29(6):652–60.
Liu S., Fukuoka M., Sakai N. 2012. Dielectric Porperties of Fish Flesh at Microwave Frequency. Food Sci Technol Res. 18 (2):157–66.
Marra F., Zhang L., Lyng J.G. 2009. Radio Frequency Treatment of Foods: Review of Recent Advances. J Food Eng. 91 (4):497–508.
Institution of Electrical, E.; Meredith R.J. 1998. Engineers' Handbook of Industrial Microwave Heating. London (UK): Institution of Electrical Engineers.
Metaxas A.C. 1996. Foundations of Electroheat: A Unified Approach. New York (NY): Wiley, Chichester.
Metaxas A.C., Meredith R.J. 1983. Industrial Microwave Heating. London (UK): P. Peregrinus on behalf of the Institution of Electrical Engineers.
Monteiro R.L., Carciofi B.A.M., Marsaioli A., Laurindo J.B. 2015. How to Make a Microwave Vacuum Dryer with Turntable. J Food Eng. 166:276–84.
Monteiro R.L., Gomide A.I., Link J.V., Carciofi B.A.M., Laurindo J.B. 2020. Microwave Vacuum Drying of Foods with Temperature Control by Power Modulation. Innovative Food Sci Emerg Technol. 65:102473.
Pianroj Y., Kerdthongmee P., Nisoa M., Kerdthongmee P., Galakarn J. 2006. Development of a Microwave System for Highly-Efficient Drying of Fish. Walailak J Sci Technol. 3(2):237–50.
Pianroj Y., Werapun W., Inthapan J., Jumrat S., Karrila S. 2018. Mathematical Modeling of Drying Kinetics and Property Investigation of Natural Crepe Rubber Sheets Dried with Infrared Radiation and Hot Air. Drying Technol. 36 (12):1436–45.
Pornchaloempong P., Sirisomboon P., Nunak N. 2012. Mass-Volume-Area Properties of Frozen Skipjack Tuna. Int J Food Prop. 15:605–12.
Pu Y.Y., Sun D.W. 2015. Vis-NIR Hyperspectral Imaging in Visualizing Moisture Distribution of Mango Slices during Microwave-vacuum Drying. Food Chem. 188:271–78.
Pu Y.Y., Sun D.W. 2016. Prediction of Moisture Content Uniformity of Microwave-vacuum Dried Mangoes as Affected by Different Shapes Using NIR Hyperspectral Imaging. Innovative Food Sci Emerg Technol. 33:348–56.
Pu Y.Y., Sun D.W. 2017. Combined Hot-air and Microwave-vacuum Drying for Improving Drying Uniformity of Mango Slices Based on Hyperspectral Imaging Visualisation of Moisture Content Distribution. Biosys Eng. 156:108–19.
Schubert H., Regier M. 2005. Microwave Processing of Food. Cambridge (UK): Woodhead Publishing.
Sevim S., Derun E., Tugrul N., Doymaz I., Kipcak A.S. 2019. Temperature Controlled Infrared Drying Kinetics of Mussels. J Indian Chem Soc. 96(9):1233–38.
Sharma G.P., Prasad S. 2001. Drying of Garlic (Allium Sativum) Cloves by Microwave–hot Air Combination. J Food Eng. 50(2):99–105.
Sosa-Morales M.E., Valerio-Junco L., López-Malo A., García H.S. 2010. Dielectric Properties of Foods: Reported Data in the 21st Century and Their Potential Applications. LWT - Food Sci Technol. 43(8):1169–79.
Zhang J., Farkas B.E., Hale S.A. 2001. Thermal Properties of Skipjack Tuna (KATSUWONUS PELAMIS). Int J Food Prop. 4(1):81–90.
Zhang J., Farkas B.E., Hale S.A. 2002. Precooking and Cooling of Skipjack Tuna (Katsuwonas Pelamis): A Numerical Simulation. LWT - Food Sci Technol. 35(7):607–16.